ASM Sc. J., 14, Special Issue 1, 2021 for ICSTSS2018, 135-142

Properties of Porous Silicon by Two-Step Alternating Current Photo-Assisted Electrochemical Etching (ACPEC) Technique under Different Applied Current Density for MSM Photodetector Device Application

Rosfariza Radzali[1]*, Muhammad Aminuddin Mohamed Azhar[1], Ainorkhilah Mahmood[2], Fatimah Zulkifli[1], Alhan Farhanah Abd Rahim[1] and Aslina Abu Bakar[1]

[1]*Faculty of Electrical Engineering, Universiti Teknologi MARA, Cawangan Pulau Pinang, 13500 Permatang Pauh, Pulau Pinang, Malaysia*

[2]*Department of Applied Sciences, Universiti Teknologi MARA, Cawangan Pulau Pinang, 13500 Permatang Pauh, Pulau Pinang, Malaysia*

The effect of different applied current density during the etching process on the properties of porous silicon (Si) structure fabricated using the two-step Alternating Current Photo-assisted Electrochemical (ACPEC) etching technique was investigated in this study. In the first step, the Si sample was etched in the electrolyte for a few minutes. This step was carried out to produce etch pits with high density on the surface of the Si sample. Following this, in the second step, the Si sample was etched using the ACPEC etching technique. From the field emission scanning electron microscopy (FE-SEM) images, the porous structure showed uniform triangular pores with an estimated size ranging between 47.9 nm and 64.1 nm. The result indicated that, the increasing current density led to the improvement of the uniformity of the porous structure and also the density of the pores. Furthermore, the surface roughness of the porous Si as measured by atomic force microscopy (AFM), increased when the applied current density increased. Subsequently, aluminium contact was deposited on non-porous and porous samples to fabricate the metal-semiconductor-metal (MSM) photodetectors. The performance of all the MSM photodetectors was investigated. The porous Si based MSM photodetectors exhibited better performance and higher current gain compared to the non-porous photodetector due to the high porosity of the porous Si that provides higher surface area to volume ratio which allows more photo detection.

Keywords: current density; MSM photodetector; porous si; two-step alternating current photo-assisted electrochemical (ACPEC) etching

I. INTRODUCTION

Silicon (Si) is a semiconductor material that is commonly used in the electronic field due to its low cost. However, silicon suffers from its weak optical properties due to its indirect band gap property (Abd Rahim *et al.*, 2016), which would reduce the performance of the device. Therefore, there is a need to improve the property of Si to obtain high performance devices. In the past years, significant advancements have been made by many research groups to understand the optical and structural properties of porous Si since Canham discovered intense luminescence in porous Si (Canham, 1990). Porous Si exhibits superior properties in comparison to the bulk Si, such as high surface area, shift of band gap and excellent luminescence intensity (Kopani *et. al.*, 2018; Praveenkumar *et al.*, 2019). Currently, porous Si has been widely used for optoelectronics and sensing applications

*Corresponding author's e-mail: rosfariza074@uitm.edu.my

(Ismail *et. al.*, 2016; Nayef, 2017; Zhang & Jia, 2017; Ge *et al.*, 2019). The structural and morphology of the porous Si that include the uniformity, porosity and density of pores can affect the electrical and optical characteristics of the devices that use porous Si semiconductor.

There are several etching techniques or methods for the fabrication of porous Si, which are dry etching and wet etching technique. The dry etching technique such as inductively coupled plasma reactive ion etching is commonly used to produce many porous structures (Kucheyev *et. al.*, 2000; Cheung *et. al.*, 2011; Hajj-Hassan *et al.*, 2011). Nonetheless, the dry etching technique has a disadvantage in which this etching technique can damage the surface of the thin film during the etching process. Therefore, this will degrade the properties of the porous structure and also the device efficiency or performance (Choi *et. al.*, 2000; Choi *et al.*, 2002). On the other hand, the wet etching technique is more preferable in the fabrication of porous Si compared to the dry etching technique because it requires simple and inexpensive equipment. From the literature, the wet etching technique that is commonly used to fabricate porous Si is electrochemical etching using direct current (DC) *(Kopani et. al., 2018*; Nayef, 2017; Dubey & Gautam, 2011). Nevertheless, this technique suffers from the formation of hydrogen bubbles during the etching process, which will eventually decrease the etching activity and result in the shallow formation of pores (Naderi, 2012). On top of that, the formation of pores is not uniformly shaped with this technique.

Therefore, in order to solve the above mentioned issues, the electrochemical etching technique using alternating current (AC) has been introduced for the formation of porous Si. So far, research works on the formation of porous Si using AC are meagre and still at an early stage. There are only few attempts made to fabricate porous Si by electrochemical etching using AC (Abd *et. al.*, 2013; Siti Nurfarhana *et al.*, 2018). In addition to that, a recent study on the formation of porous Si has been carried out by our group using a new etching technique which is two-step process of electrochemical etching using AC (Radzali *et al.*, 2017). Different etching durations have been carried out at a constant current density to investigate the properties of the resulting porous Si. From the report by Radzali *et al.* (2017), uniform and high density of porous Si structure was observed. In this two-step ACPEC etching technique, the Si sample was etched at the beginning (1_{st} step) for a few minutes. This step was carried out to produce etch pits with high density on the surface of the Si sample. After that, in the 2_{nd} step, the sample was etched in hydrofluoric acid (HF) electrolyte using alternating current photo-assisted electrochemical etching technique, which could reduce the hydrogen bubbles and allow the HF to react with the Si surface (Abd Rahim *et. al.*, 2016; Naderi, 2013).

The ability to form good porous Si structure by using the new etching technique (two-step ACPEC) has driven a motivation to apply such technique to fabricate porous Si with other etching parameters. To the best of our knowledge, the fabrication of porous Si using the new two-step ACPEC etching under different applied current density has not yet been reported. Thus, it is of interest in this work to investigate the effect of different applied current density during the etching process towards the properties of the porous Si. Then, the non-porous and porous Si based MSM photodetectors were fabricated and the characteristic or performance of the MSM photodetectors were examined and compared.

II. METHOD

N-type Si (111) with resistivity of 0.01 – 0.02 Ωcm was used in this study. The Si (111) wafer was cleaved into 1×1 cm^2 square size. The samples underwent a standard cleaning process using the Radio Corporation of America (RCA) method (Abd Rahim *et. al.*, 2016; Abd *et al.*, 2013). Porous Si samples were fabricated using the two-step ACPEC technique. Every sample was etched in a custom made Teflon cell. The etching process was performed using hydrofluoric acid (HF) based solution under the illumination of fluorescent lamp. In the first step, the sample was immersed in the solution with the mixture of HF (49%) and ethanol (95%), 1:4 by volume ratio for 5 minutes. Following this, in the second step, the silicon sample was etched using the ACPEC etching technique with the same HF and ethanol electrolyte. The silicon samples were etched under different current density: 10 mA/cm^2, 20 mA/cm^2, 30 mA/cm^2 and 40 mA/cm^2. The etching duration was fixed for 10 minutes. An etching duration of 10 minutes was chosen according to the recent study by our group on the fabrication of porous Si, in which the highest pore density and

uniform pores were obtained with this etching duration (Radzali *et al.*, 2017). Platinum wire was placed inside the Teflon cell to serve as cathode and the metal plate connected to the silicon sample acted as the anode. After the etching process, the porous Si sample was cleaned and rinsed with deionised (DI) water. Finally, the sample was left dried in ambient air for a few minutes.

The properties of samples were characterised using few characterisation tools, such as field emission scanning electron microscopy (FE-SEM), Atomic force microscopy (AFM) and High resolution X-ray diffraction (HR-XRD).

For the fabrication of non-porous and porous Si based metal-semiconductor-metal (MSM) photodetectors, aluminium (Al) contact was deposited on all the samples using sputtering system. The metal mask which was used for the MSM photodetector contacts was interdigitated contacts (electrodes) with finger width of about 230 μm. The spacing between the fingers is 400 μm and the length for each finger is ~3 mm. Each side of the electrode consists of the 4 fingers. Then, the current-voltage (I-V) characteristic was measured for all the samples. The measurement was carried out during the dark and with the presence of light condition to investigate the current gain of the MSM photodetector.

III. RESULTS AND DISCUSSION

The mechanism of the formation of porous Si structure has been proposed by several research groups (Gösele & Lehmann, 1995; Cullis *et al.*, 1997). In order for the dissolution of Si to occur, it is generally accepted that holes are required. Therefore, for n-tpye Si, the number of holes can be increased and supplied optically by illuminating the Si sample with light. The generated holes will be attracted to the surface of Si since the Si sample is positively biased and the Pt electrode is negatively biased which is placed in the HF based electrolyte. The HF based electrolyte is used for the formation of porous Si due to its properties that are able to dissolve the passivated Si surface. During the formation of the porous structure, two hydrogen atoms evolve for each Si atom dissolved. The proposed reaction during the pore formation is (Beale *et. al.*, 1985; Lehmann & Föll, 1990)

$$Si + 6HF \rightarrow H_2SiF_6 + H2 + 2H^+ + 2e^- \quad (1)$$

In addition, applying the electric current between the HF electrolyte and the Si sample during the etching process can increase the etching rate (Lehmann, 2002). Therefore, by increasing the current density, the etching activity becomes more significant and etches deeper into the Si sample which results in the increase of the pore size and the porosity of the porous Si structure. The changes in the porous Si structure as subjected to different etching current density in this study were observed in the FE-SEM images.

Figure 1 displays the FE-SEM micrographs of the non-porous and porous Si samples fabricated under different current density. Based on the 2D FE-SEM micrographs, average pore diameters were determined and the porosity of the porous samples was estimated using ImageJ software. The results are shown in Figure 2 to show the correlation between the average pore diameter and the porosity for all the porous Si samples, under different applied current density. The non-porous Si exhibited smooth and flat surface (Figure 1(a)), hence, the porosity value for this sample was not determined. However, after the etching process, the formation of pores was observed on the Si surface. Figure 1(b) exhibits the surface morphology of porous Si sample etched with 10 mA/cm² applied current density. The etching was at the initial stage with the average pore diameter measured to be 47.92 nm and the porosity was 26.65%.

Moreover, as the applied current density increased, the surface morphology underwent more substantial transformation. At 20 mA/cm² applied current density as displayed in Figure 1(c), the size of the pore and porosity increased to 48.13 nm and 40.68%, respectively. From the observation, the shape of the pores showed triangular like structure. As the applied current density was increased to 30 mA/cm² (Figure 1(d)), the porous structure became more noticeable. At this stage, the pore size and pore density are not only increased significantly, but they were accompanied by the uniform distribution of triangular like pores. We can observe that, the formation of pores was more uniform than the samples etched at 10 and 20 mA/cm² applied current density. The average pore diameter and the porosity from this sample were measured to be 58.33 nm and 41.40%, respectively. On top of that, as the applied current density was increased further to 40 mA/cm² (Figure 1(e)), the formation of uniform triangular pore can be seen throughout the sample

surface. The average pore diameter and the porosity percentage were increased with the values of 63.17 nm and 42.98%, respectively. The average pore size of porous Si samples in this work is similar to the result obtained in previous study (Abd *et al.*, 2013).

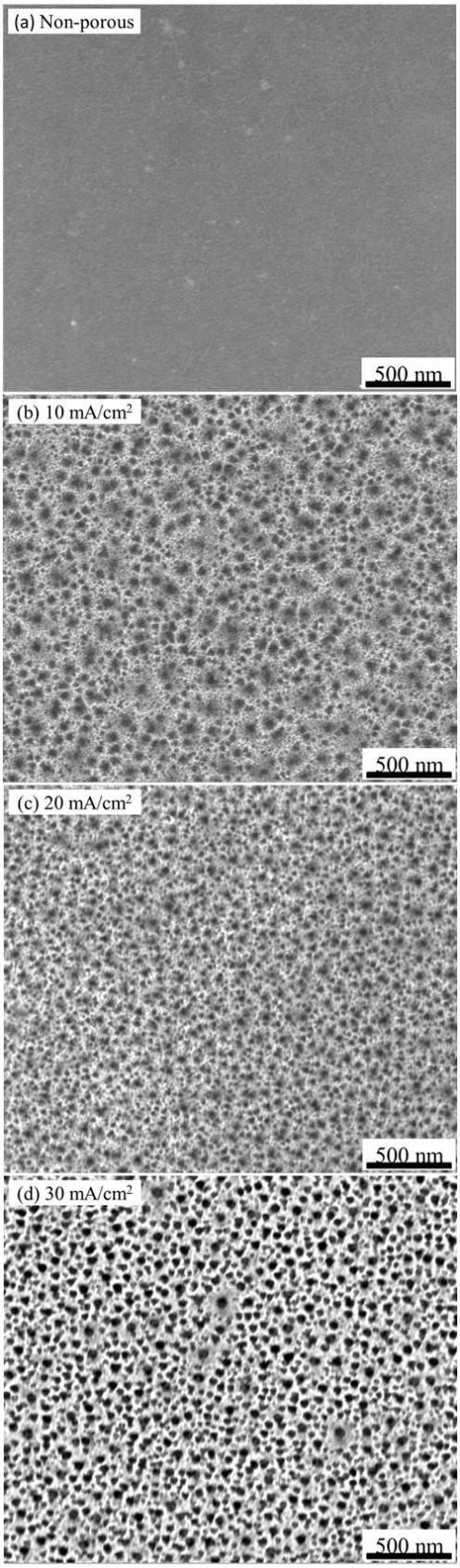

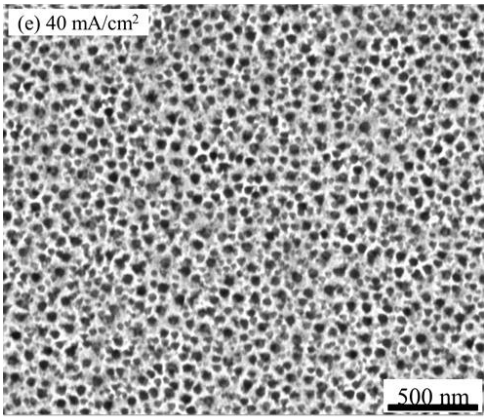

Figure 1. FE-SEM micrographs of non-porous and porous silicon samples fabricated by etching at different applied current density: (a) non-porous, (b) 10mA/cm², (c) 20mA/cm², (d) 30mA/cm², and (e) 40mA/cm²

Therefore, current density affects significantly the formation of the porous structure in which the uniformity of the porous structure, porosity, pore size and density increase with the increasing applied current density during the etching process.

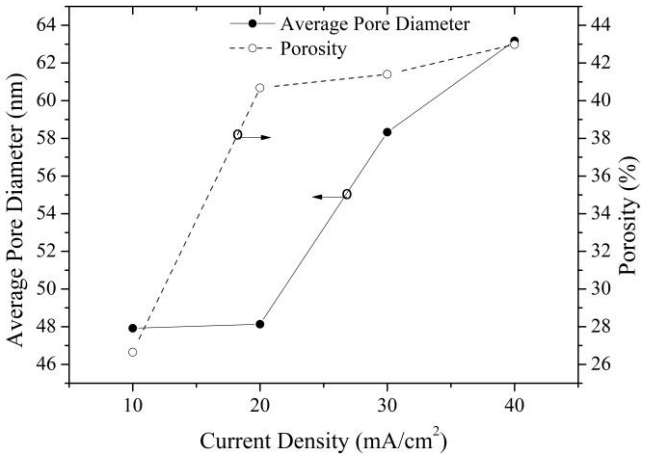

Figure 2. Dependence of average pore diameter and porosity of the samples on different current density

Figure 3 shows the AFM measurement for non-porous and porous Si samples fabricated under different applied current density. The surface roughness in root mean square (RMS) was measured within a scanned area of 5×5 μm² and the average pore depth of all the porous silicon samples was measured and estimated using section-line scan. The correlation between the surface roughness and estimation of average pore depth with respect to different current density of etching is shown in Figure 4. The non-porous sample

shows a low RMS value indicating a smooth surface, hence, the average pore depth value for non-porous Si is not included in Figure 4. However, anodisation affected the surface morphology of the silicon thin film significantly. Hence, from the result, when the applied current density during the etching process increased, the RMS roughness of the porous samples and the estimated average pore depth increased. This observation is also supported by the FESEM images (Figure 1) whereby as the applied current density increased the pore size and porosity increased which result in relatively rougher surface. A similar trend has been observed in the previous report of porous Si (Kulathuraan *et al.*, 2016). On top of that, as the applied current density increased, the etching activity increased and etched deeper into the Si sample resulting in an increased average pore depth.

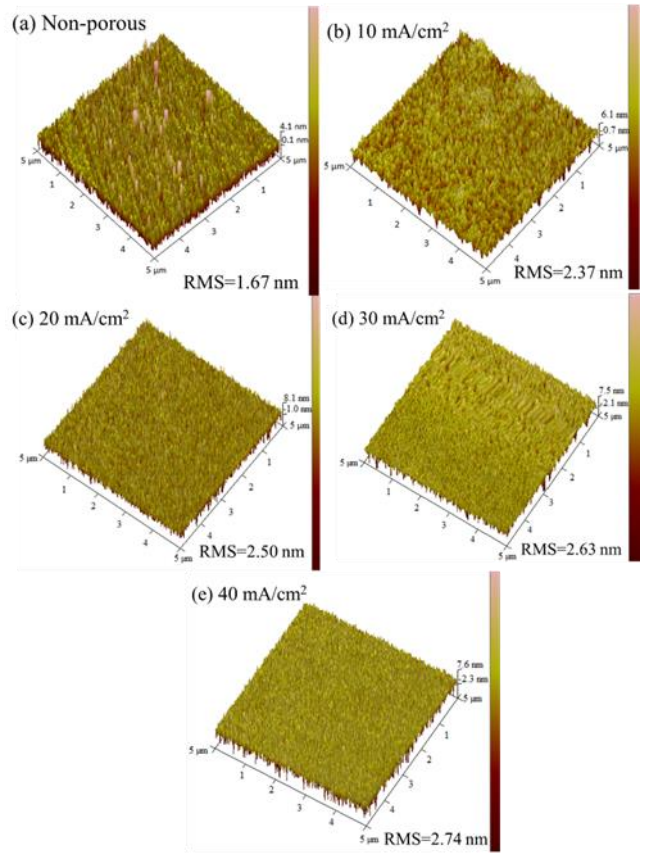

Figure 3. AFM measurement of non-porous and porous silicon samples obtained by etching at different applied current density: (a) non-porous, (b) 10mA/cm², (c) 20mA/cm², (d) 30mA/cm², and (e) 40mA/cm²

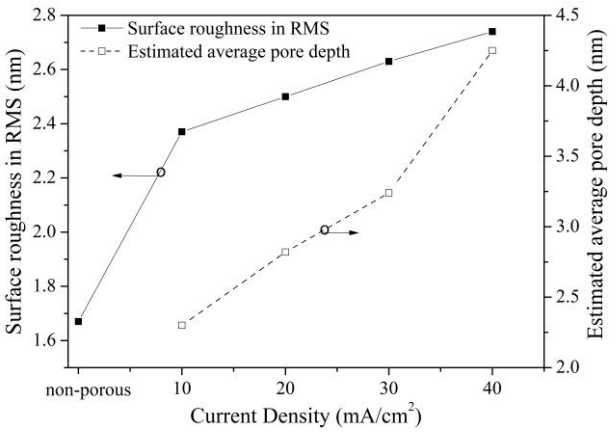

Figure 4. Relationship of surface roughness and estimated average pore depth of the samples on applied current density

HR-XRD measurement was carried out to obtain the crystalline quality and the crystallite size for all the samples. Figure 5 depicts the HR-XRD pattern for the non-porous and porous silicon samples subjected to various current density. For the non-porous Si sample, the Si (111) peak appears at 28.46°. On further observation, we found that the peak position for the porous samples was slightly shifted to lower angle relative to the non-porous sample. The shift in the peak position was related to the presence of the tensile strain on the porous samples after the etching process (Naderi, 2012).

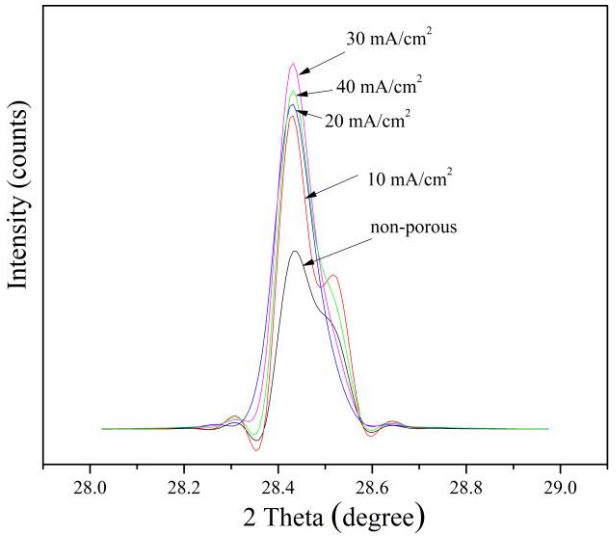

Figure 5. 2-theta scan patterns of non-porous and porous silicon samples with different current density

Furthermore, it is worth noting that the peak intensity of all the porous Si samples was higher in contrast to the non-porous Si sample and the sample etched at 30 mA/cm²

applied current density showed the highest peak intensity. On top of that, the FWHM value of porous samples was narrower than that of the non-porous sample. The higher peak intensity and narrower FWHM value suggested better crystalline structure from the uniform pore formation of the porous samples as opposed to the non-porous sample (Abd Rahim *et al.*, 2012).

Moreover, the Debye-Scherrer equation was used to calculate the average of crystallite size as shown in Equation (2).

$$D = (0.9\,\lambda)/((B\cos\theta)) \quad (2)$$

where D is the average crystallite size, λ is the incident x-ray radiation wavelength with value of 0.15406 nm, B is the FWHM value and θ is the diffraction angle in radian. The average crystallite size for non-porous was ~54.64 nm and the samples etched with current density of 20 and 30 mA/cm² showed higher value of average crystallite size with the value of ~68.30 nm. The higher value of the crystallite size for porous samples in contrast to the non-porous sample was associated to the narrowing of FWHM value in the HR-XRD pattern. However, the average crystallite size for the sample etched with 40 mA/cm² of current density slightly decreased to ~58.54 nm due to the broadening of the FWHM value. The broadening of the FWHM value could be due to the growth of native oxide on the surface of the porous structure (Young *et al.*, 1985) when etched at higher current density. The details of the HR-XRD data and the calculated crystallite size for all the samples are summarised in Table 1.

Table 1. Summary of the peak position, FWHM value and average crystallite size of non-porous and porous Si samples

Samples	2θ (°)	FWHM (°)	Average crystallite size (nm)
Non-porous	28.46	0.15	54.64
10 mA/cm²	28.46	0.15	54.64
20 mA/cm²	28.43	0.12	68.29
30 mA/cm²	28.44	0.12	68.30
40 mA/cm²	28.45	0.14	58.54

Figure 6 displays the current-voltage (I-V) characteristics of non-porous and porous Si based MSM photodetectors obtained by different current density. The samples were measured for dark current, I_{dark} under dark condition and photo current, I_{photo} under the illumination of light. All samples exhibited Schottky characteristics. From Figure 6, non-porous samples showed no response or changes upon the illumination of light in which the photo and dark current exhibited almost the same current level. On the contrary, all porous samples displayed a good response upon light illumination whereby the photo current, I_{photo} has higher current level in relative to the dark current, I_{dark}. The change of the forward current, which can be indicated as $\Delta I = I_{photo} - I_{dark}$, increased as the current density increased. Moreover, all the porous samples showed lower dark current in contrast to the non-porous samples, which resulted in higher photo response. The low dark current of the porous samples could be associated to the rough surface of the porous layer, which resulted in high resistance and eventually created high Schottky barrier (Abd Rahim *et al.*, 2016). On top of that, the pore wall of the porous structure that acted as carrier trap will increase as the porosity of the sample increased, subsequently reducing the current from passing through the porous Si layer (Abd *et. al.*, 2013; Balagurov *et al.*, 1997).

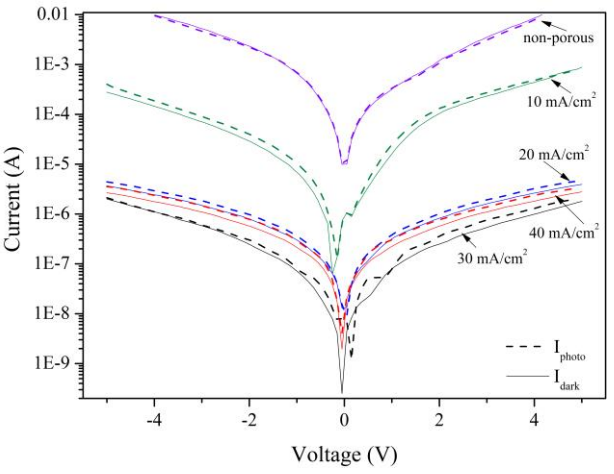

Figure 6. Current-voltage (I-V) characteristics of non-porous and porous Si based MSM photodetector obtained by different current density: 10mA/cm², 20mA/cm², 30mA/cm², 40mA/cm² when operated in the dark and under light illumination

Furthermore, the current gain for all the samples was measured to investigate the performance of the MSM photodetector. The current gain represents the photo current as a function to dark current. Figure 7 depicts the current gain for non-porous and porous Si samples under different current density which was measured at constant voltage of 4 V.

From the observation, all the porous Si based MSM photodetectors exhibited better current gain relative to non-porous Si based MSM photodetector and the current gain increased as the current density increased. Therefore, the result indicated that the porous structure has a significant effect in reducing the dark current and eventually enhancing the current gain of the porous Si based MSM photodetectors. On top of that, the uniform porous structure and high porosity of the porous Si samples provides greater surface area to volume ratio relative to the non-porous sample. Such properties allow more photo detection which in turn resulted in a higher current gain. This is supported by the AFM and FE-SEM measurements, which indicate that the porous Si samples have high surface roughness and they increased in porosity with applied current density.

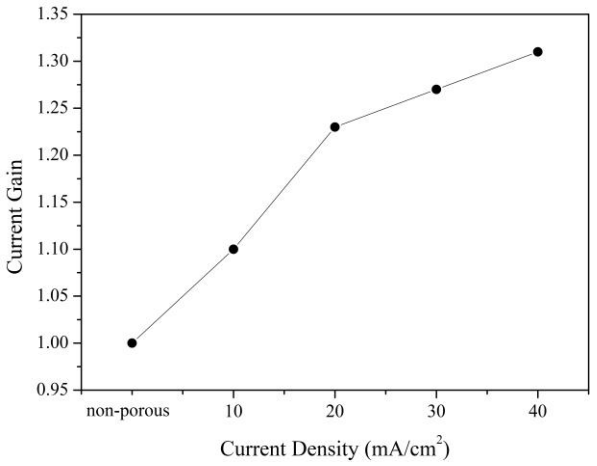

Figure 7. Current gain of non-porous and porous Si based MSM photodetector obtained by different current density

IV. CONCLUSION

In this study, we successfully fabricated uniform and high porosity of porous Si structure using the new two-step ACPEC etching technique. The porous Si structure developed uniform porous structure and higher porosity, pore density, pore size, and surface roughness with increased applied current density compared to non-porous Si. Then, we have investigated the effectiveness of uniform porous Si for MSM photodetector device application. The porous Si based photodetector exhibited better current gain compared to the non-porous Si photodetector and the current gain was observed to be increased as the current density increased. The results indicate the potential of using this new two-step ACPEC etching technique to fabricate uniform and high porosity porous structure for better performance of MSM photodetector application. For future work, other etching parameters can be varied during the etching process to produced better porous Si structure in terms of the uniformity of the pores. The porous Si can be applied to other sensing device applications such as gas sensor and solar cell.

V. ACKNOWLEDGEMENT

The authors are gratefully acknowledge the support from Universiti Teknologi MARA (UiTM) for the completion of this work. The technical support from INOR lab, Universiti Sains Malaysia is also dully acknowledged and much appreciated.

VI. REFERENCES

Abd Rahim, AF, Abdullah, MS, Mahmood, A, Ali, NK & Zahidi, MM 2016, 'Quantum confinement of integrated pulse electrochemical etching of porous silicon for metal semiconductor metal photodetector', Materials Science Forum, vol. 846, pp. 245-255.

Abd Rahim, AF, Hashim, MR, Rusop, M, Ali, NK & Yusuf, R 2012, 'Room temperature Ge and ZnO embedded inside porous silicon using conventional methods for photonic application', Superlattices and Microstructures, vol. 52, no. 5, pp. 941-948.

Balagurov, LA, Yarkin, DG, Petrovicheva, GA, Petrova, EA, Orlov, AF & Andryushin, SY 1997, 'Highly sensitive porous silicon based photodiode structures', Journal of Applied Physics, vol. 82, no. 9, pp. 4647-4650.

Beale, MIJ, Benjamin, JD, Uren, MJ, Chew, NG & Cullis, AG 1985, 'An experimental and theoretical study of the formation and microstructure of porous silicon', Journal of Crystal Growth, vol. 73, no. 3, pp. 622-636.

Canham, LT 1990, 'Silicon quantum wire array fabrication by electrochemical and chemical dissolution of wafers', Applied Physics Letters, vol. 57, no. 10, pp. 1046-1048.

Cheung, MCK, Roche, PJR, Hajj-Hassan, M, Kirk, AG, Mi, Z & Chodavarapu, VP 2011, 'Controlling optical properties and surface morphology of dry etched porous silicon',

Journal of Nanophotonics, vol. 5, no. 1, pp. 053503-053503-10.

Choi, HW, Chua, SJ, Raman, A, Pan, JS & Wee, ATS 2000, 'Plasma-induced damage to n-type GaN', Applied Physics Letters, vol. 77, no. 12, pp. 1795-1797.

Choi, HW, Chua, SJ & Tripathy, S 2002, 'Morphological and structural analyses of plasma-induced damage to n-type GaN', Journal of Applied Physics, vol. 92, no. 8, pp. 4381-4385.

Cullis, AG, Canham, LT & Calcott, PDJ 1997, 'The structural and luminescence properties of porous silicon', Journal of Applied Physics, vol. 82, no. 3, pp. 909-965.

Dubey, RS & Gautam, DK 2011, 'Porous silicon layers prepared by electrochemical etching for application in silicon thin film solar cells', Superlattices and Microstructures, vol. 50, no. 3, pp. 269-276.

Ge, D, Shi, J, Wei, J, Zhang, L & Zhang, Z 2019, 'Optical sensing analysis of bilayer porous silicon nanostructure', Journal of Physics and Chemistry of Solids, vol. 130, pp. 217-221.

Gösele, U & Lehmann, V 1995, 'Light-emitting porous silicon', Materials Chemistry and Physics, vol. 40, no. 4, pp. 253-259.

Hajj-Hassan, M, Cheung, MC & Chodavarapu, VP 2011, 'Ultra-thin porous silicon membranes fabricated using dry etching', Micro & Nano Letters, vol. 6, no. 4, pp. 226-228.

Abd, HR, Y. Al-Douri, Ahmed, NM & Hashim, U 2013, 'Alternative-current electrochemical etching of uniform porous silicon for photodetector applications', International Journal of Electrochemical Science, vol. 8, no., pp. 11461-11473.

Ismail, RA, Kadhim, RG & Abdulridha, WaM 2016, 'Effect of multiwalled carbon nanotubes incorporation on the performance of porous silicon photodetector', Optik - International Journal for Light and Electron Optics, vol. 127, no. 19, pp. 8144-8152.

Kopani, M, Mikula, M, Kosnac, D, Vojtek, P, Gregus, J, Vavrinsky, E, Jergel, M & Pincik, E 2018, 'Effect of etching time on structure of p-type porous silicon', Applied Surface Science, vol. 461, pp. 44-47.

Kucheyev, SO, Williams, JS, Jagadish, C, Zou, J, Craig, VSJ & Li, G 2000, 'Ion-beam-induced porosity of GaN', Applied Physics Letters, vol. 77, no. 10, pp. 1455.

Kulathuraan, K, Mohanraj, K & Natarajan, B 2016, 'Structural, optical and electrical characterisation of nanostructured porous silicon: effect of current density', Spectrochimica Acta Part A: Molecular and Biomolecular Spectroscopy, vol. 152, pp. 51-57.

Lehmann, V 2002, 'Electrochemistry of silicon: instrumentation, science, materials and applications', Wiley-VCH, Wenham.

Lehmann, V & Föll, H 1990, 'Formation mechanism and properties of electrochemically etched trenches in n - type silicon', Journal of The Electrochemical Society, vol. 137, no. 2, pp. 653-659.

Naderi, N 2013, 'Development of silicon and silicon carbide nanostructures for photonic applications', PhD thesis, Universiti Sains Malaysia.

Naderi, N & Hashim, MR 2012, 'Effect of surface morphology on electrical properties of electrochemically-etched porous silicon photodetectors', Int. J. Electrochem. Sci., vol. 7, pp. 11512–11518.

Nayef, UM 2017, 'Improve the efficiency of UV-detector by modifying the Si and porous silicon substrate with ZnS thin films', Optik - International Journal for Light and Electron Optics, vol. 130, pp. 441-447.

Praveenkumar, S, Lingaraja, D, Mahiz Mathi, P & Dinesh Ram, G 2019, 'An experimental study of optoelectronic properties of porous silicon for solar cell application', Optik, vol. 178, no., pp. 216-223.

Radzali, R, Zakariah, MZ, Mahmood, A, Rahim, AFA, Hassan, Z & Yusof, Y 2017, 'The effect of ecthing duration on structural properties of porous Si fabricated by a new two-steps alternating current photo-assisted electrochemical etching (ACPEC) technique for MSM photodetector', in AIP Conference Proceedings, vol. 1875, no. 1, pp. 020003.

Siti Nurfarhana, S, Zainuriah, H, Naser Mahmoud, A, Lim Way, F & Quah Hock, J 2018, 'Effect of different UV light intensity on porous silicon fabricated by using alternating current photo-assisted electrochemical etching (ACPEC) technique', Journal of Physics: Conference Series, vol. 1083, no. 1, pp. 012034.

Young, IM, Beale, MIJ & Benjamin, JD 1985, 'X-ray double crystal diffraction study of porous silicon', Applied Physics Letters, vol. 46, no. 12, pp. 1133-1135.

Zhang, H & Jia, Z 2017, 'Application of porous silicon microcavity to enhance photoluminescence of ZnO/PS nanocomposites in UV light emission', Optik - International Journal for Light and Electron Optics, vol. 130, pp. 1183-1190.